Journal of Computational Neuroscience 14, 311–327, 2003

No Parallel Fiber Volleys in the Cerebellar Cortex: Evidence from Cross-Correlation Analysis between Purkinje Cells in a Computer Model and in Recordings from Anesthetized Rats

DIETER JAEGER
Department of Biology, Emory University, Atlanta, GA 30322, USA
djaeger@emory.edu

Received September 6, 2001; Revised November 27, 2002; Accepted December 13, 2002

Action Editor: Steve Redman

Abstract. Purkinje cells aligned on the medio-lateral axis share a large proportion of their ∼175,000 parallel fiber inputs. This arrangement has led to the hypothesis that movement timing is coded in the cerebellum by beams of synchronously active parallel fibers. In computer simulations I show that such synchronous activation leads to a narrow spike cross-correlation between pairs of Purkinje cells. This peak was completely absent when shared parallel fiber input was active in an asynchronous mode. To determine the presence of synchronous parallel fiber beams in vivo I recorded from pairs of Purkinje cells in crus IIa of anesthetized rats. I found a complete absence of precise spike synchronization, even when both cells were strongly modulated in their spike rate by trains of air-puff stimuli to the face. These results indicate that Purkinje cell spiking is not controlled by volleys of synchronous parallel fiber inputs in the conditions examined. Instead, the data support a model by which granule cells primarily control Purkinje cell spiking via dynamic population rate changes.

Keywords: cerebellum, temporal coding, modeling, rat, in vivo, excitation, inhibition

Introduction

The cerebellum has been noted for its involvement in the precise control of movement at a temporal precision of less than 10 ms (Ivry, 1997; Timmann et al., 1999). Such precise control of movement likely requires control of spiking in cerebellar cortex of the same precision. One mechanism underlying such precision has been proposed to consist of the activation of 'beams' of parallel fibers (Sasaki and Strata, 1967; Eccles et al., 1967; Braitenberg, 1967; Garwicz and Andersson, 1992). This hypothesis states that synchronously activated bundles of parallel fibers trigger Purkinje cell spiking for precise temporal control of movement. The amount of shared parallel fiber inputs has been estimated to exceed 50% of the total excitatory synapses (Napper and Harvey, 1988) for cells located in close proximity. Each parallel fiber runs for about 5 mm along a cerebellar folium (Harvey and Napper, 1991), therefore most of the shared excitation is preserved for several hundred Purkinje cells aligned on the medio-lateral axis. This amounts to sharing tens of thousands of parallel fibers between these Purkinje cells, because each cell receives ∼175,000 such inputs (Napper and Harvey, 1988).

The cross-correlation technique is commonly used to determine the degree of functional connectivity between pairs of neurons recorded in vivo (Perkel et al., 1967; Moore et al., 1970; Aertsen et al., 1989; Vaadia et al., 1995; Johnson and Alloway, 1996). A narrow central peak in a cross-correlogram indicates that neurons are spiking in synchrony, and thus may belong to a neural assembly that is coactivated during information processing. Such coactivated sets of neurons are

effective signals in signal propagation. Since Purkinje cells are inhibitory, the net effect of a synchronous population event would be an effective suppression of spiking in the deep cerebellar nuclei.

To examine the control of Purkinje cell spiking by synchronous parallel fiber inputs I used computer simulations with a detailed Purkinje cell model. This model reveals that a small proportion of synchronously active parallel fibers can drive Purkinje cells to precisely timed spikes. Asynchronously timed parallel fiber inputs did not induce correlated Purkinje cell spiking, however, even when 100% of parallel fiber input was shared between two cells. To establish the actual mode of parallel fiber function in vivo, dual recordings from Purkinje cells were obtained in anesthetized rats. A complete absence of spike synchrony between Purkinje cells was found, indicating that parallel fibers operate in an asynchronous mode in the examined conditions.

Methods

Computer simulations were performed using the Genesis software package (Bower and Beeman, 1994) under the Linux operating system. A detailed compartmental Purkinje cell model was taken unaltered from previous work (De Schutter and Bower, 1994a). This model includes a realistic set of active conductances so that the model replicates active responses to current injection recorded in vitro. Excitatory inputs were simulated as AMPA-type conductances with a reversal potential of 0 mV, and a time course of a dual exponential alpha function with rise/fall time constant of 0.5/1.2 ms that matches experimental data (Barbour, 1993). The peak conductance was 0.7 nS, which is increased by 3–5 times from the unitary conductance measured in vitro (Barbour, 1993). Inhibitory inputs consisted of $GABA_A$-type conductances with a reversal potential of −80 mV and rise/fall time constants of 1.6/9.3 ms. Each presynaptic element was simulated as a random time series of activation times (Jaeger et al., 1997). The number of synaptic inputs was taken from previous work (Jaeger et al., 1997), and included 1,474 excitatory parallel fiber synapses and 1,695 inhibitory stellate cell synapses. Except when otherwise noted, all excitatory synapses were activated randomly at a mean rate of 37 Hz, and all inhibitory synapses at a mean rate of 1.5 Hz. The excitatory input rate used was much higher than likely to be present in vivo (Huang et al., 1993), which partly compensates for the reduced number of these inputs present in the model (De Schutter and Bower, 1994b). This input pattern leads to a total synaptic conductance with a high tonic component and fluctuations that are much more pronounced for inhibitory than excitatory inputs (Fig. 1a and b in Jaeger and Bower, 1999). The response characteristics of the model cell to this synaptic input pattern were previously characterized in detail (Jaeger et al., 1997) and the same inputs were tested with dynamic clamping in vitro (Jaeger et al., 1999). The model has a stable resting membrane potential at −68 mV, but upon depolarization by an external input it generates inward plateau currents supporting a depolarized up-state and intrinsic pacemaker activity even when the external input ceases. During ongoing synaptic input consisting of a baseline of excitatory and inhibitory synaptic inputs the cell is stabilized in the depolarized up-state, and the synaptic inputs modulate the balance of intrinsic plateau currents (Jaeger and Bower, 1997). It should be noted that a single parallel fiber input in the model is expected to be equivalent to 3–5 such inputs in vivo, as the time course of EPSCs matched experimental data, but the unitary amplitude was increased by a factor in the range of 3–5. Thus, the synchronous activation of 147 parallel fiber synapses in the model (10% of all modeled synapses) corresponds to the synchronous activation of 450–750 parallel fibers in vivo (less than 0.5% of the roughly 175,000 parallel fiber synapses a single Purkinje cell receives). In the present study, simulated synchronous volleys of inputs in the model were always delivered in a distributed fashion across the entire dendritic tree. A previous study using this model showed that for synchronous inputs of moderate size the somatic response is similar for distributed and clustered input patterns (De Schutter and Bower, 1994c), and this issue was not further pursued in the present study.

To determine whether observed cross-correlations for the Purkinje cell model were dependent on its intrinsic cell properties, the same set of input patterns was also tested with a generic one-compartment model. This model had a membrane resistance of 63.7 MegΩ, a membrane capacitance of 314 pF, and a leak reversal potential of −80 mV as parameters, leading to a passive time constant of 20 ms. To simulate active properties, Na^+ and K^+ spike currents, and an A-current were included, and the density was adjusted to yield spike frequencies matching the Purkinje cell model for the default input pattern (Fig. 1b, d). The kinetics for the three active currents were taken from the Purkinje cell model. The resulting model had a stable resting

potential at −80 mV, and showed a spike threshold of 0.35 nA current injection. Spike frequency increased from 29 to 79 Hz for a range of 0.4 to 1.0 nA current injection. The time course of synaptic input conductances to the single compartment model was exactly identical to those used in the Purkinje cell model. This was achieved by activating the same set of simulated synaptic elements, but focusing the output of all synapses on the single compartment. The relative conductance amplitudes of all synapses were maintained, but the unitary conductance amplitude was reduced by a factor of 3.3. This scaling was performed so that the relation between passive input resistance and synaptic conductance was the same for the Purkinje cell and single compartment models. The purpose of this single compartment model was to evaluate the role of specific Purkinje cell properties in the production of output spike correlations given specific input correlations. These properties include the effect of dendritic attenuation and delays, and the interaction of synaptic input with active properties such as plateau currents and calcium dynamics. All of these properties were absent in the single compartment model, which thus contrasts Purkinje cell processing with the most basic integration of synaptic conductances in a spiking compartmental model.

In vivo recordings were obtained from crus IIa of anesthetized rats. All use of rats complied with the NIH guidelines on the care and use of laboratory animals and were approved by the local Institutional Animal Care and Use Committee. The details of the surgical procedures used to expose crus IIA of cerebellar cortex have been described in previous publications (Jaeger and Bower, 1994). Briefly, male Sprague-Dawley rats of 60–90 day age were anesthetized by intraperitoneal injection with ketamine (75 mg/kg), acepromazine (0.75 mg/kg), and xylazine (3.9 mg/kg). Touchup doses of 1/3 of this amount of anesthetic were given when light paw withdrawal reflexes developed, usually occurring at intervals of 1 hour. The body temperature was maintained at 35–36°C. and the heart rate was monitored. The cerebellar cortex was surgically exposed and kept covered with light mineral oil to prevent drying of the brain surface. Tungsten microelectrodes of 2–6 MegΩ impedance (A-M systems, Inc.) were inserted to a depth of 150 to 250 μm until spikes of single Purkinje cells could be isolated. The signal was band-pass filtered between 1 and 3,000 Hz and digitized at 10 kHz for analysis. Spike separation was performed off-line with a window discrimination routine that is based on peak amplitude and spike width separation. The quality of cell isolation was checked by the presence of a refractory period in the interspike-interval histograms. Simple spikes and complex spikes were not separated, and in most cells a small number of short duration intervals resulted from the discrimination of multiple simple spikes within a complex spike (see Fig. 7).

Dual recordings of Purkinje cells were aligned parallel to the visible rostral and caudal boundaries of crus IIa, which has a width of approximately 1 mm. Since the typical parasagittal dendritic extent of a Purkinje cell is 0.25 mm, about 4 non-overlapping Purkinje cell dendritic fields span the width of the crus IIa surface. The alignment of recording electrodes was accurate within 50 μm with respect to boundaries of crus IIa based on graticule readings taken with a binocular surgical microscope. Distances between recording electrodes along the parallel fiber axis ranged between 0.05 and 1.5 mm based on graticule readings. Thus, the dendritic alignment of recorded Purkinje cell pairs would provide a large number of common parallel fiber inputs based on anatomical arguments. To ascertain that parallel fibers were not rendered inactive due to surgical exposure, Purkinje cells were tested for responses to electrical stimulation at the top of the molecular layer. Stimuli consisted of bipolar current pulses of 0.1 ms duration and 0.1–0.5 mA amplitude applied with a tungsten microelectrode. The stimulation electrode was located at the same distance from the boundary of crus IIa as the recorded Purkinje cells, and was typically placed 500 μm lateral to Purkinje cell recordings. To drive Purkinje cell spiking with peripheral stimulation, trains of air-puffs (one 50 ms puff every 250 ms) were applied to the upper lip via a glass pipette with an opening of 1 mm pointed at the skin from a distance of 1–3 mm. Each air-puff resulted in a visible indentation of a small skin area. At the end of an experiment the rat was euthanized by giving a lethal dose of sodium pentobarbital i.p.

Cross-correlation analysis was carried out with the same C-routines for experimental and simulated data. The y-axis of the histograms was normalized so that each bin shows the event count per second of recorded data in the time slice represented by the bin width. Standard deviations for cross-correlograms of spontaneous activity were computed across 50 repetitions of the cross-correlation after shuffling the interspike intervals of one spike train. Standard deviations for cross-correlograms of air-stimulus driven activity

were computed from repeated stimulus presentations ($n > 50$) after subtracting the PSTH predictor following established methods (Palm et al., 1988; Brody, 1999).

Results

Modeling of Neural Responses to Shared Asynchronous or Synchronous Excitation

The goal of this modeling study was to test different simulated parallel fiber input patterns that are fully or partially shared between Purkinje cells for their ability to induce cross-correlation peaks. Simulations with shared input patterns were run serially with the same realistic Purkinje cell model, and in addition with a generic one-compartmental model (see Methods). Cross-correlations were computed from 30 s of spiking activity, corresponding to approximately 1,200 spikes.

Because of the large proportion of shared input fibers expected for Purkinje cells aligned on the parallel fiber pathway, the first input condition that was tested consisted of 100% of shared excitatory inputs between 2 simulations. In contrast, inhibitory inputs to Purkinje cells aligned on the parallel fiber pathway originate from different interneurons because their axons run perpendicular to the parallel fibers (Palkovits et al., 1971). Therefore, an asynchronous random background of firing of inhibitory inputs is not shared between Purkinje cells. When we tested for cross-correlation in the absence of parallel fiber volleys we therefore set the asynchronous inhibitory input as uncorrelated, while varying the correlation of asynchronous excitatory inputs. When two simulations received all excitatory inputs at exactly the same times (100% correlation), but synapses were activated individually in an asynchronous mode, the resulting cross-correlation was completely flat (Fig. 1c). This result can be explained by the inability of many asynchronous excitatory inputs to trigger spikes with fine temporal precision, which we have previously reported for the Purkinje cell model and with simulated synaptic input in vitro (Jaeger et al., 1997; Jaeger and Bower, 1999). This is due to the fact that a large number of uncorrelated inputs leads to only very small temporal fluctuations on top of a constant tonic conductance (Fig. 1a). Even in the case of the single compartment simulation, correlated spiking was absent for this input pattern (Fig. 1e). This indicates that the properties of the asynchronous excitatory input pattern per se rather than the special active properties of Purkinje cells lead to the lack of cross-correlation. In the case of a large number of randomly occurring small excitatory inputs, even 100% of shared excitatory inputs between cells does not lead to an appreciable amount of cross-correlation. This result generalized over different output spike rates (10–100 Hz) elicited by different rates of excitatory input, and over different ranges in the rate of excitation and inhibition balanced to produce similar spike rates. This balance occurs always when the amplitude of the inhibitory conductance is bigger than the amplitude of excitatory conductance (Fig. 1a) so that the inhibitory and excitatory synaptic current are of the same amplitude at a membrane potential of around −40 mV (Jaeger et al., 1997).

Due to the significant effect of even single inhibitory inputs on Purkinje cell spiking (Jaeger et al., 1997; Häusser and Clark, 1997) simulations with shared asynchronous inhibition but completely different excitatory input patterns showed a large cross-correlation peak (Fig. 2). This peak reached significance, even when only 50% of the inhibitory inputs were shared. The single compartment simulation showed similar results, though the cross-correlation peak was somewhat narrower (Fig. 2). Shared inhibition of this type might be expected for neighboring Purkinje cells as they may be contacted by the same population of inhibitory interneurons.

Synchronicity in the activity of many excitatory inputs would be an expected consequence of most schemes of temporal coding that have been proposed for cerebellar cortex (Braitenberg et al., 1997) or other structures (Abeles, 1991; Riehle et al., 1997; Singer, 1999; Diesmann et al., 1999). Therefore input patterns that contained an increasing number of synchronously activated excitatory inputs were tested for their ability to lead to the expression of cross-correlation peaks. The same statistics for the activation of single inputs as described above were used, but an increasing number of excitatory inputs were activated with identical timing. This resulted in the emergence of a central peak in the cross-correlation between simulations that shared the same population of synchronously activated inputs. For the Purkinje cell simulation, around 100 synchronously activated excitatory inputs were required before the cross-correlation peak was significant (Fig. 3b, c). This input pattern leads to clearly recognizable peaks in the excitatory input conductance for each synchronous input volley (Fig. 3a). The single compartment model showed a highly significant peak already with 73 synchronized inputs (Fig. 3e), but not with 37

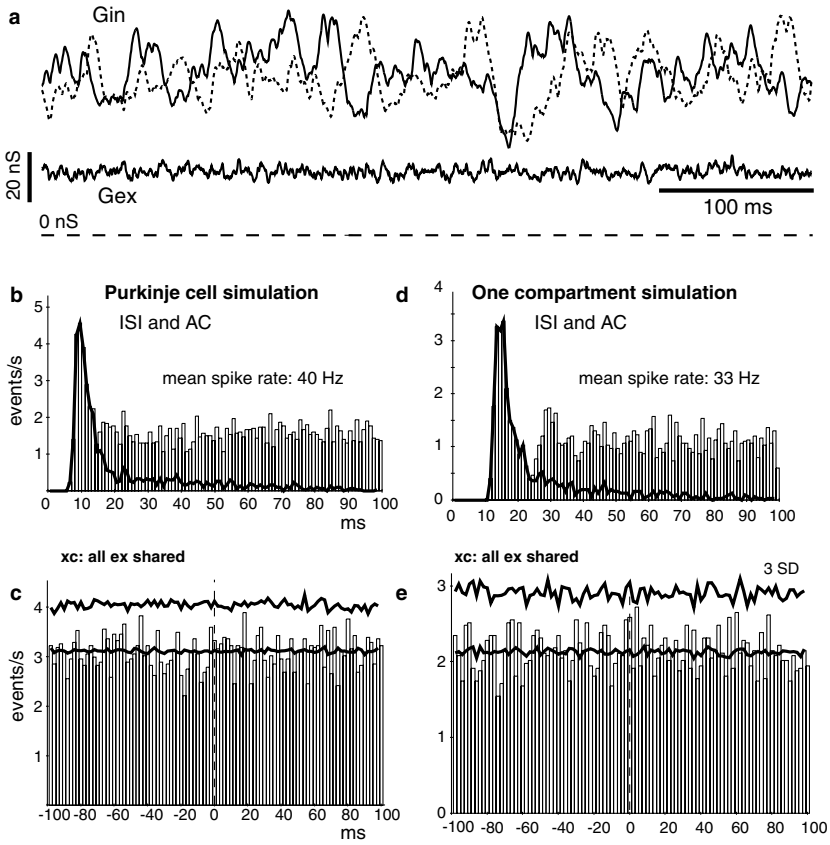

Figure 1. Compartmental models show an absence of synchronous activation when subjected to 100% shared asynchronous excitation. (a) The inhibitory (Gin) and excitatory (Gex) synaptic input conductance with the input pattern used. Gex was identical between pairs of simulations, whereas Gin was uncorrelated (dotted trace). (b) Interspike interval (ISI) histogram (black line) and autocorrelation (vertical bars) of the spike pattern shown by a detailed Purkinje cell simulation in response to simulated shared asynchronous parallel fiber and stellate cell input. (c) When two simulations share an identical pattern of parallel fiber inputs that occur in a random asynchronous fashion there is no resulting spike synchrony. The inhibitory input was uncorrelated between the two simulations and effectively led to a decorrelation of output spiking. (d) ISI histogram and autocorrelation of the spike pattern in the single compartmental model in response to the same input pattern. (e) The cross-correlation function for the one-compartmental model shows evidence of a very weak correlation of the spike activity with 100% of shared excitatory inputs. The binwidth is 2 ms for all histograms. The lower solid line denotes the mean expected correlation value for each bin based on shuffle prediction (see Methods) and the upper solid line denotes 3 standard deviations from the mean. A value of 1 event/s for a bin signifies that cell 2 fired on average once per second at this delay from cell 1 spikes. Event counts are proportional to the bin size.

(not shown). These results indicate that the Purkinje cell with its strong intrinsic currents, calcium dynamics, and large dendrite require more synchronized inputs than an isopotential compartment with few active currents to express a cross-correlation peak, but only by a factor of about two. The number of 100 synchronous inputs in my simulations is equivalent to 300–500 synchronous parallel fiber inputs in vivo (see methods), and thus only corresponds to about 0.3% of 175,000 parallel fiber synapses a Purkinje cell actually receives. These results therefore demonstrate that synchronicity in a very small proportion of parallel fibers in vivo should suffice to generate precise spike correlations in Purkinje cells sharing these inputs.

A cross-correlation analysis can pick up spike events due to synchronous inputs as a peak only if they occur frequently enough so that the number of events per second exceeds the random variability in the cross-correlation bin count. For my simulations the cross-correlation of shared synchronous events was significant when they occurred at least at a rate of 4 event/s (see confidence limits in Figs. 1–3). This value was confirmed by examining cross-correlations for simulations with different rates of shared synchronous

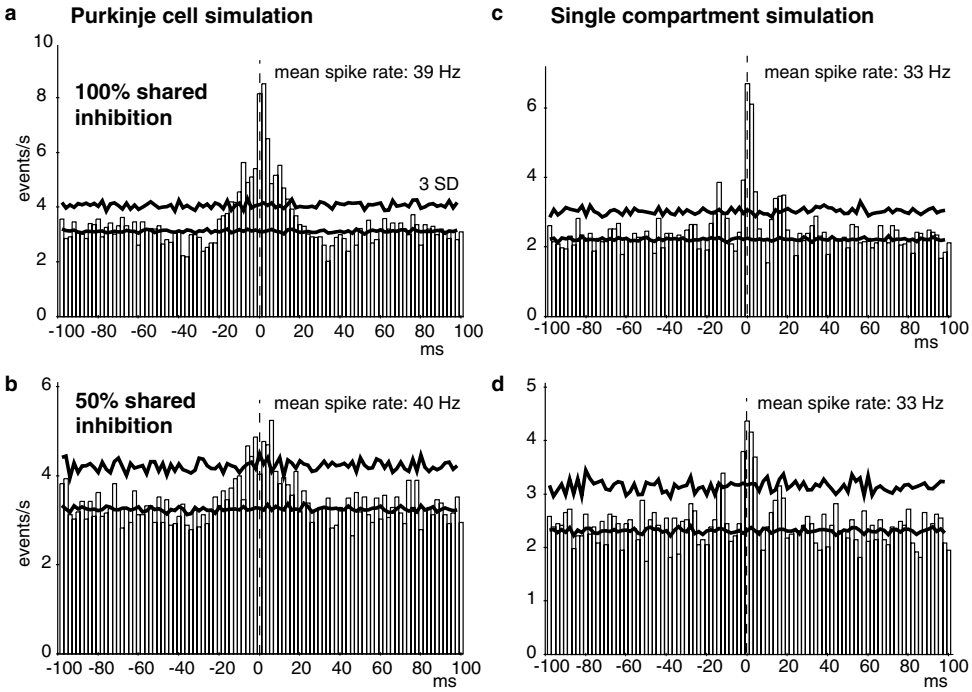

Figure 2. Common asynchronous inhibition leads to significant synchronous spiking. When the same input properties as shown in Fig. 1 were used, but the asynchronous inhibitory inputs were shared while the pattern of excitatory inputs was completely different, a significant narrow peak emerged in the cross-correlations. Though inhibition per se does not trigger spikes, spike synchronization occurs here due to synchronous releases of inhibition. (b) Even 50% of shared inhibitory inputs still lead to input events of sufficient amplitude to synchronize postsynaptic spiking. (c, d) Synchronization in the single compartment simulation occurs at a similar frequency as in the Purkinje cell, but is temporally more precise.

input events, which produced significant peaks when 4 events/s were exceeded (data not shown). The number of synchronous events needed to show significance is a function of the spike rate, which is on average 35 Hz in anesthetized and also in awake rats (Savio and Tempia, 1985; Stratton et al., 1988). It is also a function of the length of the recorded data set, as longer data sets show a reduced standard deviation in the cross-correlation bin counts, and thus can show significance for a smaller density of synchronous spikes caused by parallel fiber volleys. The number of spikes analyzed in my simulations (>1000) is usually considered sufficient to show physiologically relevant cross-correlations, however. Simultaneous recordings of larger cell populations can also show significant synchronous events at a low rate, because random synchronized spikes among a larger cell population are very unlikely. Such rare events have in fact been detected in multiple Purkinje cell recordings, and were shown to be caused by synchronous climbing fiber inputs (Lang et al., 1999).

Synchronicity of parallel fiber inputs is not likely to be absolutely precise in vivo because of variable parallel fiber conduction velocities and because granule cells may not be activated at exactly the same time even if the parallel fiber system was used for temporal coding. Therefore the input patterns with 147 synchronous inputs (Fig. 3c, f) were modified to include temporal dispersion (jitter) among the synchronously activated population of parallel fibers. It was found that jitter of the synchronous input led to a broadening of the cross-correlation peak by the same amount as the introduced jitter (Fig. 4). Thus, when the individual inputs in a synchronous population were randomly jittered by ± 5 ms, the cross-correlation peak was also jittered by ± 5 ms (Fig. 4b, e). Purkinje cell simulations showed a broader peak compared to a single compartment simulation even in the absence of any input jitter (Fig. 4a). This effect is likely due to the spatial distribution of parallel fiber inputs in the large dendritic tree of the Purkinje cell model, and subsequent dendritic processing. Such processing includes passive dendritic conduction delays and attenuation as well as synaptically triggered transients in voltage gated currents in this model (Jaeger et al., 1997; De Schutter, 1998).

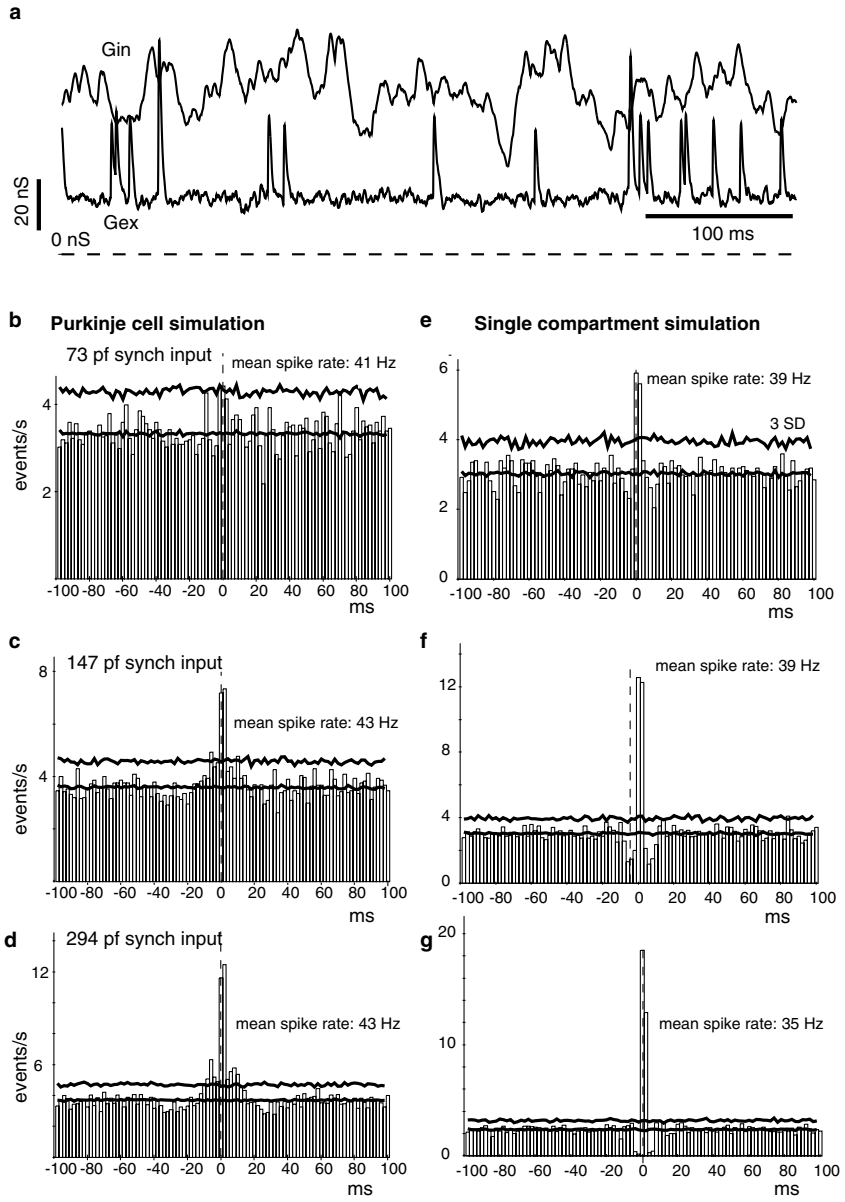

Figure 3. Synchronized excitatory inputs lead to a strong spike correlation in both models. (a) The input conductances for the synchronous activation of 147 parallel fibers at 37 Hz on top of an asynchronous baseline (Gex), and the asynchronous baseline of inhibition (Gin) are shown. Each activation of a parallel fiber volley leads to a clear peak in Gex. (b–d) Responses of the Purkinje cell model for simulations with increasing synchrony in the shared excitatory input. When 147 parallel fibers of the simulated inputs are synchronized, a highly significant narrow central peak emerges in the cross-correlation. The inhibitory input is identical to the simulations shown in Fig. 1. (e–g) Same input patterns for the one-compartment model. This model already shows a strong central peak for 73 synchronized parallel fibers (5% of total input population in the model). The binwidth is 2 ms for all histograms.

In addition to exciting Purkinje cells, synchronous parallel fiber volleys are also likely to activate inhibitory interneurons along the activated path. Thus, a synchronous inhibitory input could be coupled with direct Purkinje cell excitation along activated parallel fiber bundles. To examine whether such synchronous inhibitory inputs might lead to distinct cross-correlation peaks or interfere with the peaks expected

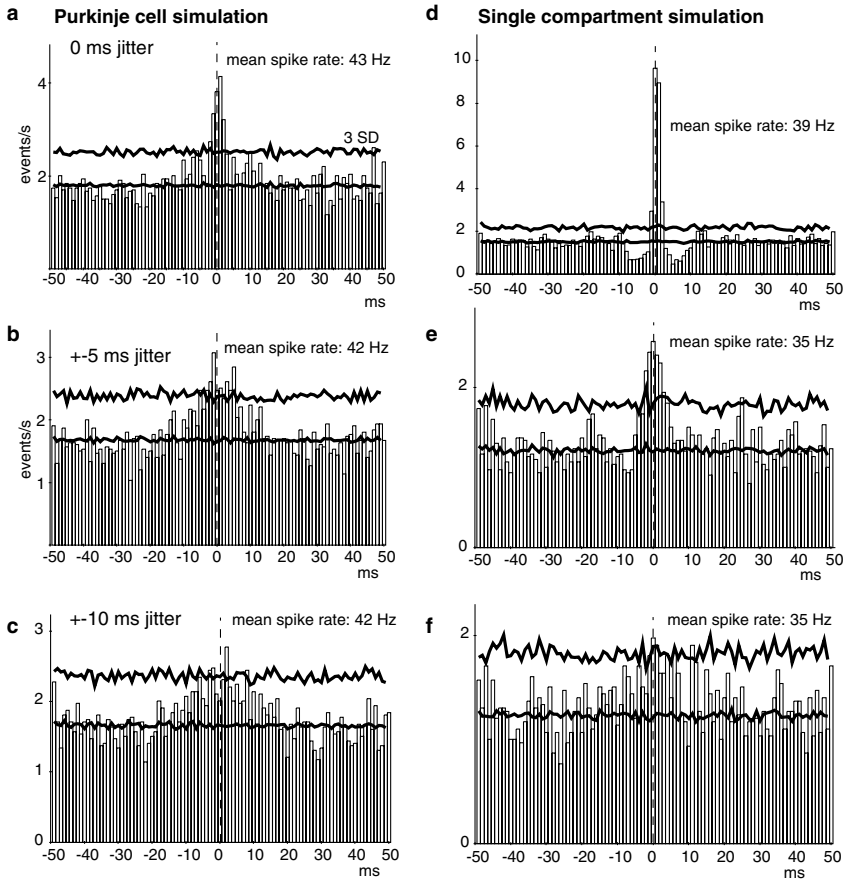

Figure 4. Temporal jitter between synchronized inputs leads to a broadening of the output spike correlation by the jitter time. (a–c) Cross-correlograms of simulated Purkinje cell responses for input patterns with 147 synchronous parallel fiber activation with increasing amount of temporal jitter. (d–f) Responses of the single compartment model to the same input patterns. The binwidth is 1 ms.

to occur as a result of excitation, several sets of simulations exploring coupling between excitation and inhibition were performed. As a baseline, simulations contained 20 synchronous parallel fiber events per second, which by itself led to a sharp peak centered on zero (Fig. 5a, d). Then, synchronous inhibitory inputs for different numbers of inhibitory synapses were tested without synchronous excitation. The response for all but very small synchronous inhibitory inputs consisted of a broad 20–50 ms center peak in the cross-correlogram (Fig. 5b, e). Physiologically, this case of synchronous inhibition alone corresponds to parallel fiber volleys activating interneurons off-beam to the recorded Purkinje cells. Inhibitory interneurons have a projection zone at a 90-degree angle to the parallel fibers and are thus expected to transmit off-beam lateral synchronous inhibition upon receiving a parallel fiber volley. However, strong on-beam components of synchronous inhibition are also expected at a slight delay from a parallel fiber volley. This case was tested with synchronous parallel fiber excitation followed at 1–5 ms with synchronous inhibition. A range of combinations of intensity and delay of synchronous excitation and inhibition was simulated. All conditions led to similar cross-correlation peaks consisting of a primary narrow peak indicating the synchronous excitation, and a surrounding broader flank (Fig. 5c, f). The origin of these peaks is further elucidated in Fig. 6, which shows Purkinje cell simulation results for a strong synchronous parallel fiber excitation followed 1 ms later by a strong synchronous inhibition. The raw data traces (Fig. 6a) show that synchronous inputs (arrows) typically produced a spike response followed by a pause, except during periods of high frequency spiking (no pause), or hyperpolarization (no spike). The cross-correlation can pull out these different events, when the

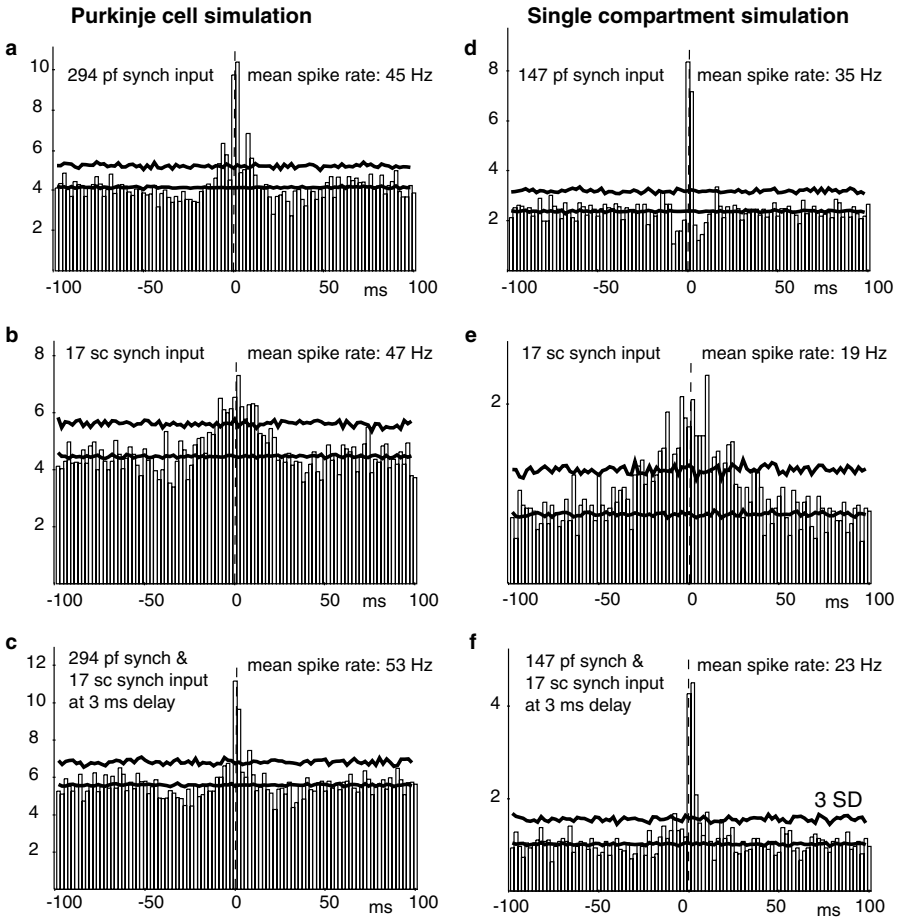

Figure 5. The impact of synchronous inhibitory events. (a, d) The top panels show the cross-correlation due to synchronous excitatory inputs from 294 parallel fibers in the Purkinje cell or 147 parallel fibers in the single compartment. These numbers were chosen to generate a comparable strong peak for both models in this baseline condition (see Fig. 3). The rate at which these synchronous inputs occurred was reduced from 37 to 20 Hz compared to previous simulations (Fig. 3), to allow simulating synchronous inhibitory input at the same rate without depressing the overall spike rate too far. (b, e) Synchronous inhibitory input was delivered through 17 stellate cell (sc) synapses (about 1% of the total inhibitory inputs a Purkinje cell receives), in the absence of synchronous excitation. This led to a 50 ms wide peak similar to the case of 50% asynchronous shared inhibition (Fig. 2). (c, f). Synchronous inhibitory events (17 synapses) were coupled to the synchronous excitatory inputs shown in (a, d) at a delay of 3 ms. The resulting correlations are similar to the case of pure excitatory synchronization, with a reduced representation of the broad peak seen with pure inhibitory synchronization.

spikes contributing to the cross-correlation histogram are limited based on the inter-spike interval following each spike. Spikes that are followed by a pause have a much higher probability of being synchronized precisely between a simulated pair (Fig. 6e) than spikes that are not followed by a pause (Fig. 6d). Finally, the case of synchronous inhibition slightly preceding synchronous excitation was also investigated. Only when the inhibition was very strong (2% of inputs or more) could it fully suppress spikes caused by synchronous excitation. This case could be physiologically relevant, as deep parallel fibers that preferentially may contact basket cells are bigger and thus have a faster conduction velocity than more superficial parallel fibers (Ito, 1984).

In vivo Cross-Correlation of Purkinje Cells Along the Parallel Fiber Pathway

Extracellular recordings were obtained from pairs of Purkinje cells ($n = 30$) along the parallel fiber pathway at distances between 0.1 and 1.5 mm in anesthetized rats. The median distance was 0.5 mm. The

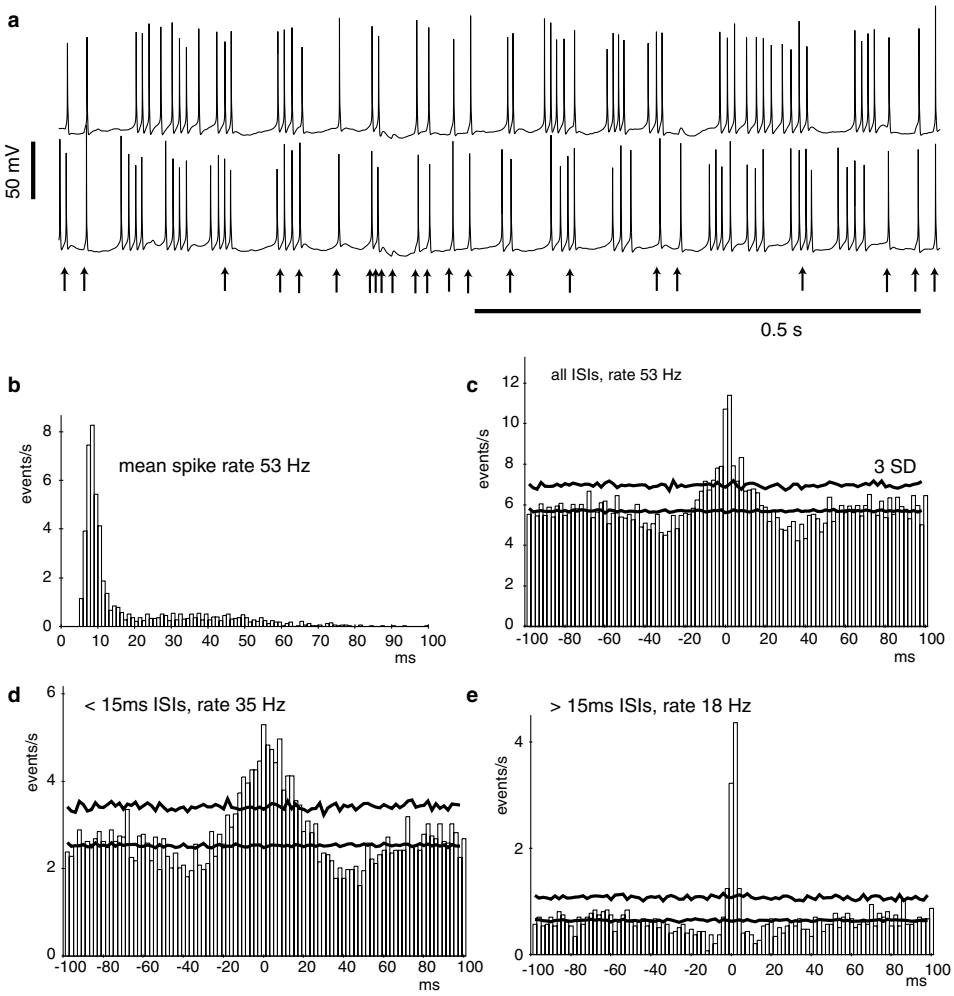

Figure 6. Analysis of the spike—pause pattern resulting from coupled excitatory and inhibitory input volleys. The example of synchronous inhibition following synchronous excitation by 1 ms is examined in detail for the Purkinje cell simulation. (a) A 1 s segment of the raw data shows that synchronous events (indicated by arrows) typically led to a spike followed by a pause. (b) The mean spike rate of this simulation was comparable to the simulations without such synchronous events. To keep the overall rate of inputs a cell receives similar to the case without synchronous inputs, the rate of random background excitation was reduced from 37 to 35 Hz, and inhibition from 1.5 to 1.2 Hz. (c) The cross-correlation for all spikes consists of a large 4 ms narrow peak surrounded by a 30 ms flank. This is nearly identical to the result with a 3 ms delay between excitation and inhibition (Fig. 5c), illustrating that the precise delay in this range is not crucial. (d, e) The cross-correlation was constructed separately for spikes preceding long (>15 ms) or short (<15 ms) intervals. This condition was imposed on both spike trains before the remaining spikes were cross-correlated. The results show that the precise narrow peak can be picked out by selecting intervals preceding a pause, whereas the broader flank is likely due to spikes induced by synchronous events during periods when the model was in a fast spiking regime.

mean spike rate of the recorded population of Purkinje cells ($n = 40$) was 53 ± 25 Hz. The range of spontaneous spike rates was 25–95 Hz, except one neuron firing at 18 Hz, and one at 163 Hz. The pattern of spiking was irregular, with small pauses that rarely exceeded 100 ms (Figs. 7a, b and 8a, b). The spontaneous activity pattern was stable over the duration of the recording for all neurons. To determine the amount and precision of synchronous spiking in this spontaneous activity the cross-correlation between each pair of simultaneously recorded neurons was computed. The results showed that there was not a single narrow (<10 ms) peak in the cross-correlograms obtained ($n = 30$). Most cross-correlograms of spontaneous activity were completely flat (Fig. 7e). The lack of precise spike synchronization was not due to a disruption or conduction block of the parallel fiber pathway, since in all cases tested ($n = 21$) both cells had clear responses to electric shock

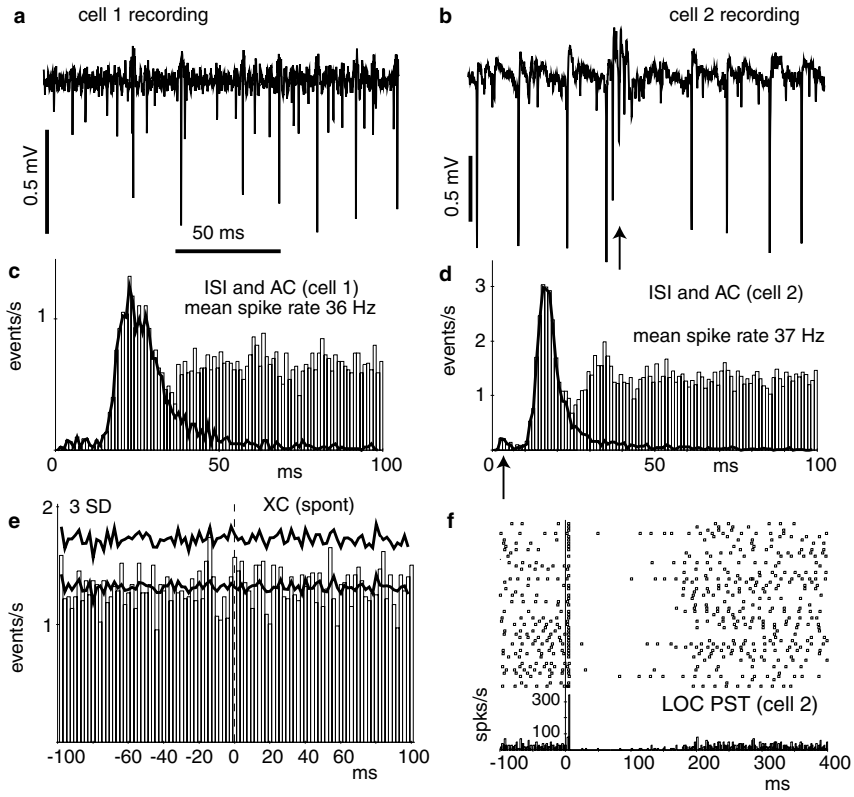

Figure 7. Synchronous spiking is absent along the parallel fiber pathway during spontaneous Purkinje cell activity. (a, b) Extracellular spike recordings digitized at 10 kHz of two cells recorded at a distance of 100 μm along the parallel fiber pathway. A single cell can be clearly discriminated in each recording. The arrow in (b) points to climbing fiber input, which typically elicited a brief spike burst. Climbing fiber inputs occurred at an average rate of less than 1 Hz. (c, d) ISI distribution shown as solid line superimposed on the autocorrelation (AC) histogram for the same cells. The flat AC histogram indicates an absence of oscillatory activity. The arrow in (d) points to the short intervals due to spike bursts occurring in response to climbing fiber inputs. Except for climbing fiber responses the ISI distribution is very similar to the modeling results with random background input. (e) The cross-correlation between these two cells was flat, indicating the absence of any correlation in the spike activity. The binwidth is 2 ms. (f) Responses to direct electrical parallel fiber stimulation (LOC). Repetitions of the stimulus are aligned at time 0 and spike trains are depicted as raster histogram. A long lasting inhibition was the most common response, which was in some cases preceded by a short-latency spike response. Note that a feedforward activation of on-beam basket cells by parallel fibers is well suited to suppress a spike response via dendritic parallel fiber input. Labeling and analysis methods are identical to modeling results.

stimulation of the parallel fiber pathway at a single site (Fig. 7f). These responses always had a strong inhibitory component, as expected from the activation of inhibitory interneurons by parallel fiber volleys. Some pairs recorded showed a broad correlation peak with a width of 50–200 ms (10/30 pairs, Figs. 8c and 9c). Bins surrounding the peaks were often still above baseline but failed to reach the significance criterion of 3 standard deviations. These broad peaks were distributed between pairs recorded at all distances between 0 and 1000 μm, with the most frequent occurrence coinciding with the most dense sampling of pairs, which was obtained at 500 μm. To elucidate the origin of these broad peaks, the cross-correlation analysis was split up between spikes preceding short intervals and spikes preceding long intervals. As indicated by the simulation results, peaks due to synchronous inhibitory inputs should be most apparent when only spikes followed by a pause are sampled. In contrast, the experimental results show that the broad cross-correlation peaks were fully accounted for by spikes occurring during high-frequency firing (Fig. 8c). The cause for this peak is apparent from the raw data traces upon closer inspection (Fig. 8a), as periods of high-frequency firing in both neurons are loosely synchronized. It has been demonstrated that such periods of coincident firing rate changes lead to central cross-correlation peaks (Brody, 1999).

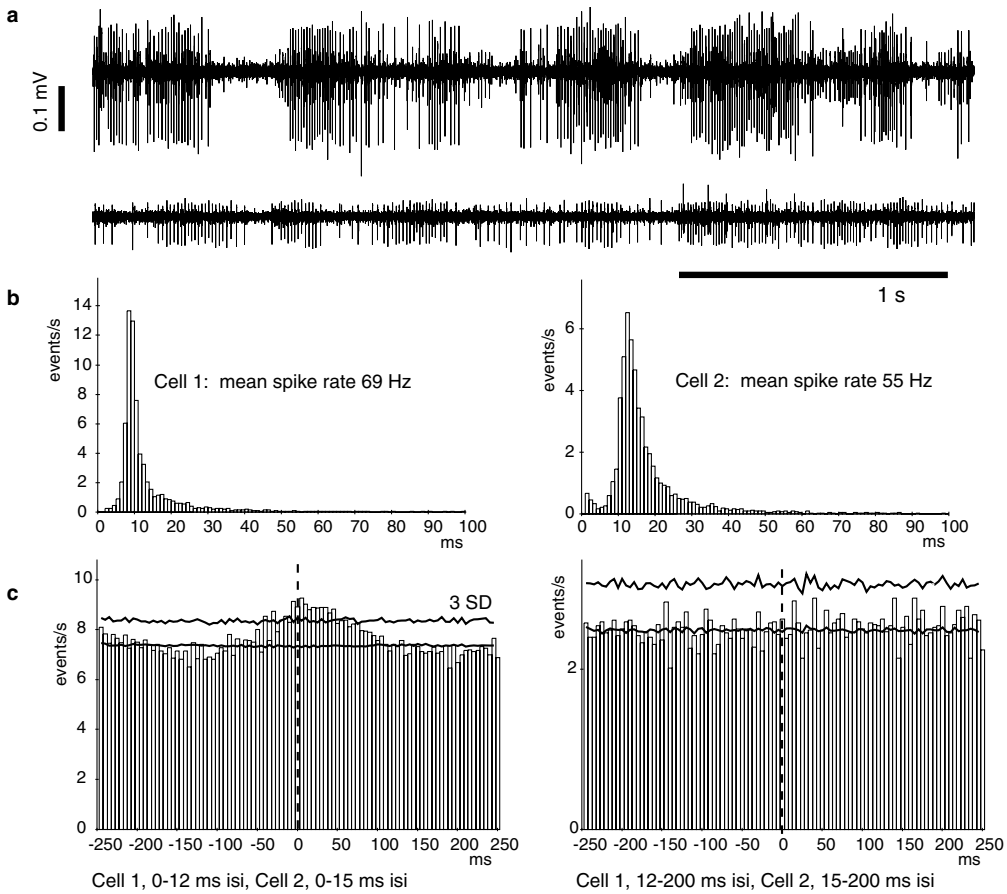

Figure 8. Analysis of broad cross correlation peaks during spontaneous activity. An example of a pair that was classified as having a significant broad cross-correlation peak is examined in detail. These two cells were recorded at a distance of 0.5 mm distance along the parallel fiber path. (a) A 3 s segment of the raw data traces reveals periods of high frequency spiking that are loosely shared between both neurons. (b) The ISI distributions are very comparable to the model results shown above, except for the small number of short intervals induced by climbing fiber input (see Fig. 7). (c) The cross-correlation was split up between short intervals and long intervals for each neuron by splitting the ISI distribution at the onset of the tail (12 ms for cell 1, 15 ms for cell 2) analogous to the processing of modeling results shown in Fig. 6. In contrast to the modeling of synchronous events the cross-correlation peak here is fully caused by spikes with short succeeding intervals. This excludes the case of common pauses due to synchronous inhibition for causing the observed peak.

Since specific signals may be absent in the parallel fiber pathway during spontaneous activity, the cross-correlation analysis was repeated for activity obtained during sensory stimulation that resulted in a strong modulation in the observed spike activity (Fig. 9a, b). Even when both cells showed strong ongoing modulation in spiking with a train of air-puff stimuli to the face ($n = 20$), the cross-correlation showed no additional peak of common activation at a short time scale (Fig. 9d). This result indicates that the modulation in spiking caused by sensory input is not mediated by synchronously activated parallel fiber beams, because the computer simulations showed that even a small percentage of synchronous parallel fiber activation results in a narrow cross-correlation peak. Parallel fibers have a conduction speed around 0.3–0.5 m/s (Crepel et al., 1981), and thus at distances between 0.1 and 1.5 mm a conduction delay between 0.2 and 5.0 ms can be expected. If a particular 'beam' of activated parallel fiber signal excited one of my recorded Purkinje cells strongly at a given time, a noticeable activation of the second recorded cell would therefore be expected shortly before or after. Even though parallel fibers have a range of conduction velocities, the expected dispersion of a strong signal along the recorded distances would be less than 2 ms, and a narrow cross-correlation

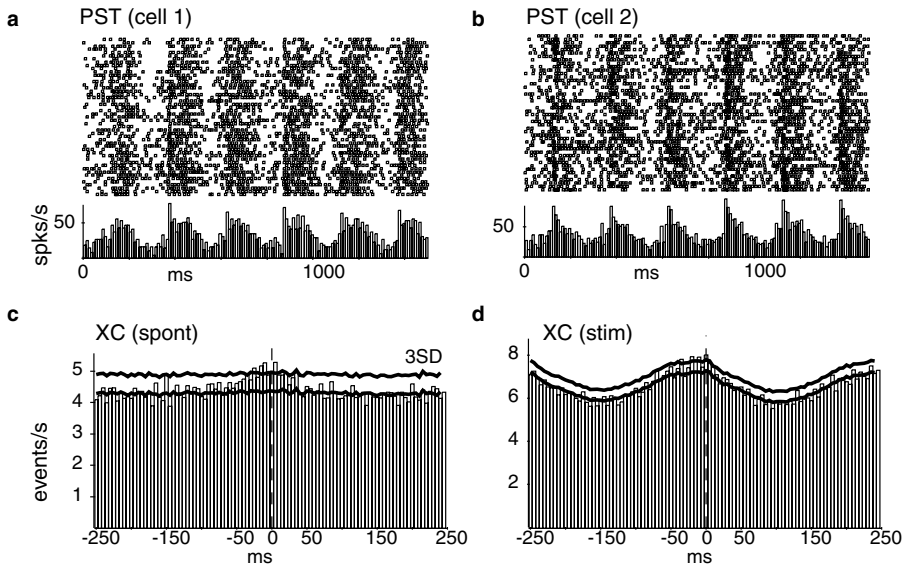

Figure 9. Stimulus driven spike responses of Purkinje cells are not associated with synchronous spiking along the parallel fiber pathway. (a, b) Stimulus aligned spike rasters for two Purkinje cells recorded simultaneously at a distance of 500 μm along the parallel fiber pathway. A strong common modulation of the spike rate driven by a train of air puff stimuli to the face is seen in both cells. Air puffs were repeated at intervals of 250 ms. (c) The cross-correlation of these two cells during spontaneous spiking shows an example of weak coactivation on the timescale of 50 ms. The binwidth is 5 ms. The lower horizontal line shows the expected bin count when no correlation is present, and the upper line shows a level of 3 standard deviations away from the baseline. (d) The raw cross-correlation during the stimulus driven activity is shown as vertical bars. The expected cross-correlation baseline is shown by the lower horizontal line. It is wavy because of common response components to the stimulation. The contribution of the common stimulus response components were computed by the PSTH predictor method (Palm et al., 1988). The upper horizontal line depicts the 3 standard deviation mark, above which cross-correlations were deemed to significantly depart from the expected baseline.

peak ($<$10 ms) would be seen. Thus, the strong spike modulation seen in vivo with sensory input appears to be due to asynchronous granule cell population activity.

Discussion

Ideas regarding the computational algorithm taking place in cerebellar cortex have focused on temporal coding because the function of the cerebellum is implicated in the fine temporal control of movement (Houk et al., 1996; Ivry, 1997; Mauk et al., 1998; Timmann et al., 1999). The parallel fiber system has been viewed as particularly well suited to convey temporal coding by means of volleys of activity along parallel fiber 'beams' (Braitenberg and Atwood, 1958; Eccles et al., 1967; Garwicz and Andersson, 1992; Braitenberg et al., 1997). In my simulations about 100 synchronous parallel fiber inputs occurring at frequencies of only 4 events/s were expressed as narrow peaks in Purkinje cell cross-correlations. In vivo this corresponds to 300–500 synchronous parallel fiber inputs (0.3% of total input population) as each synapse in the model was 3–5 times stronger than the physiological amplitude to allow for a reduced total input population (see methods). The cross-correlation peaks were conserved in the presence of temporal jitter in the synchronous inputs expected from variable parallel fiber conduction velocities. The number of 100 parallel fiber inputs was shown to be sufficient to trigger a spike in Purkinje cells in slices from 14 day old rats (Barbour, 1993), supporting the concept that a very small proportion of synchronously active parallel fibers will be expressed in precisely timed spike outputs. The number of 300–500 needed synchronous inputs indicated by my simulations was likely higher than 100 because the simulated barrage of ongoing asynchronous background input acts as a significant shunt not present in slice recordings, and reduces the effect of synaptic input on the soma (Rapp et al., 1992; Jaeger et al., 1997). The similarity of the cross-correlation results between the full Purkinje cell model and the isopotential single-compartment model that lacked most of the voltage-gated Purkinje cell conductances indicates

that it was the correlation structure and size of the inputs and not specific Purkinje cell processing that caused the observed spike synchronization. The only detectable contribution of detailed properties of the Purkinje cell model consisted of a small degree of spike desynchronization and a small increase in detection threshold in response to synchronized inputs. These simulation results lead to the clear prediction that even small volleys of synchronously activated parallel fibers should lead to precisely time-locked spiking of Purkinje cells along the parallel fiber trajectory. Even if as many as 90% of parallel fiber synapses had a weight of zero (silent synapses), as recently suggested (Isope and Barbour, 2001), only 3% of parallel fibers would need to be synchronously active to induce time-locked Purkinje cell spiking. These effects are not likely to be obscured by inhibitory inputs triggered by parallel fiber activity, as in most cases inhibitory inputs would occur at a small delay. The simulation results show that such coupled inhibitory inputs do not disrupt cross-correlation peaks, but are visible as correlated pauses.

The present experimental results showed that synchronous parallel fiber volleys did not control Purkinje cell spiking in our in vivo preparation to a significant degree, because a narrow spike correlation between Purkinje cells along the parallel fiber trajectory was absent. A similar result has been reported before for Purkinje cell correlations in decerebrated cats (Ebner and Bloedel, 1981), supporting the generality of this finding. The only cross-correlation study showing positive correlations between Purkinje cells (Bell and Grimm, 1969) had a total of 5 recorded pairs, all of which were separated by less than 0.1 mm. Thus, shared inhibition due to local interneurons can easily explain the peaks shown for 3 pairs in this paper, which is likely to be enhanced under the condition of the pentobarbital anesthesia employed. The absence of narrow cross-correlation peaks I found for pairs separated by wider distances indicates that the large majority of Purkinje cell spikes are not triggered by synchronous parallel fiber volleys, since such volleys would activate Purkinje cells along the active parallel fiber bundle and thus lead to spike synchronization. Because Purkinje cells along a parallel fiber bundle receive a large proportion of their excitatory inputs from the same axons, the expected result of a parallel fiber volley is shared excitation of all aligned Purkinje cells. Thus, even a small sample of recorded pairs should reveal this type of activity. The concept of a parallel fiber volley as a timing mechanism requires that the volley be synchronized within a very narrow window of at most a few ms and spread along the parallel fiber pathway. The activity found in our preparation is not consistent with this model. A lack of Purkinje cell activation along parallel fiber beams has recently also been observed with voltage-sensitive dye imaging in the isolated guinea pig brain (Cohen and Yarom, 1998).

It is important to distinguish between synchronous volleys of activity and less synchronized bursts as well as phasic and tonic rate changes of granule cell and parallel fiber activity. The 50–200 ms peaks in the cross-correlations found in this study are well accommodated by the hypothesis that fast Purkinje cell rate changes are driven by preceding bursts in the granule cell layer. The observation that the broad peaks seen were selectively associated with periods of increased Purkinje cell spike rates (Fig. 8) supports this hypothesis. A recent set of studies in awake behaving rats supports the notion that granule cells in awake animals show ongoing strong asynchronous modulation of spiking (Hartmann and Bower, 1998, 2001). The strong oscillatory population activity in granule cells found in the quiet awake state in these studies would be exactly the predicted input pattern driving the correlated Purkinje cell rate changes that underlie the observed broad cross-correlation peaks. In fact, similar oscillatory bursting is present in the granule cell layer of ketamine anesthetized rats as the anesthesia gets a little lighter before a renewed injection (Jaeger, unpublished observation). In behaving rats, granule cell responses in crus IIa were most dominant with tactile stimulation, and not movement (Hartmann and Bower, 2001). These responses consisted of pronounced population bursts that would again be the predicted input pattern for the Purkinje cell activation I found with air puff trains in the anesthetized rat.

My findings on the absence of temporal coding in the parallel fiber input to Purkinje cells may appear at odds with the involvement of cerebellum in precise movement timing. Temporal precision, however, could be mediated by other components of the cerebellar circuitry. The activation of climbing fiber inputs to populations of Purkinje cells along the parasagittal plane has been found to be synchronous (Welsh et al., 1995) and may contribute to temporal coding in the cerebellum. These synchronous climbing fiber events occur at frequencies of <1 Hz, however, and are thus not well suited to control a significant proportion of Purkinje cell spikes (Lang et al., 1999).

The ascending granule cell axons may provide an alternate way to provide temporally exact stimuli (Llinás, 1982; Bower, 1997a, 1997b). This view is supported by data showing that Purkinje cells are primarily activated in response to tactile stimuli by granule cell activity directly below, and not by parallel fiber beams (Bower and Woolston, 1983). Although such ascending inputs are not expected to yield precisely synchronized Purkinje cell output, the rapid change in spike activity of a patch of Purkinje cells appears of temporally sufficient precision to act as a timing signal. In addition, these data showed strong inhibitory responses to tactile stimulation, which may also be involved in the control of behavioral timing, because pauses of Purkinje cell spiking effectively trigger spikes in the deep cerebellar nuclei (Gauck and Jaeger, 2000). If ascending granule cell inputs are primarily responsible for driving well-timed phasic responses in Purkinje cells, the role of the parallel fiber system might be that of modulating these responses to bring the context of inputs to surrounding somatotopic areas to bear on the ongoing computation. A recent modeling study showed that an increase in the level of parallel fiber activity is in fact likely to change the timing and amplitude of responses to ascending inputs (Santamaria et al., 2002).

The control of Purkinje cell spiking is likely influenced by long-term depression that eliminates the responses of Purkinje cells to specific synaptic inputs. The idea of training Purkinje cells to pause at specific times due to LTD was first proposed by Albus (1971). A detailed model of how such pauses could be adaptively timed during delayed eye-blink conditioning has recently been published (Medina and Mauk, 2000), demonstrating that a cerebellar timing machine can be constructed without the need for synchronous parallel fiber volleys. Interestingly, this model can create precisely timed output without the need of generating parallel fiber volleys. Instead, granule cell responses to a given stimulus are required to show many different temporal profiles, and the precise timing of the climbing fiber as a teaching signal imparts the trained temporal coding of Purkinje cell responses.

Purkinje cell activity recorded in awake behaving animals consistently shows dynamically timed fast and slow modulations of spike rate on top of a tonic background of fast irregular spiking. Different areas in cerebellar cortex show selective responses for smooth pursuit (Lisberger and Fuchs, 1978) and saccadic (Mano et al., 1991) eye movements, wrist movements (Mano and Yamamoto, 1980), and reaching movements (Fortier et al., 1989). Many of these responses are directly related to sensory feedback during movement such as slip of a hand-held object (Dugas and Smith, 1992). The tonic baseline of 20–150 Hz of spiking found in these studies is similar to the activity found in the present study under ketamine anesthesia. Computer simulations (Jaeger et al., 1997) using the Purkinje cell model also employed here, and a dynamic clamp study (Jaeger and Bower, 1999) showed that this activity is well explained by an ongoing background of granule cell activity, which stabilizes the inward plateau currents of Purkinje cells in the up-state. In contrast, the absence of such a baseline of ongoing inputs is often associated with a pronounced bistability in Purkinje cell spiking in vitro (Llinás and Sugimori, 1980; Williams et al., 2002) and animals under pentobarbital anesthesia (Bell and Grimm, 1969). The dynamic modulation of Purkinje cell spiking during behavior is in agreement with the hypothesis that rapid granule cell activity changes are translated into adaptive Purkinje cell responses via learning algorithms. The present study supports this framework of a dynamic regulation of Purkinje cell activity by granule cells in the absence of specific synchronous parallel fiber volleys. Future work will need to further clarify the relative role of parallel fibers, ascending granule cell axons, and inhibitory interneurons in the expression of precisely timed changes in Purkinje cell activity during behavior.

Acknowledgments

The author thanks Drs. Hagai Bergman and Douglas Falls for critical comments, and Dr. James Bower for supporting preliminary experiments leading to this study. This work was supported by NIMH R29MH-57256.

References

Abeles M (1991) Corticonis: Neural Circuits of the Cerebral Cortex. Cambridge University Press, New York.

Aertsen AM, Gerstein GL, Habib MK, Palm G (1989) Dynamics of neuronal firing correlation: Modulation of "effective connectivity". J. Neurophysiol. 61: 900–917.

Albus JS (1971) A theory of cerebellar function. Math. Biosci. 10: 25–61.

Barbour B (1993) Synaptic currents evoked in Purkinje cells by stimulating individual granule cells. Neuron. 11: 759–769.

Bell CC, Grimm RJ (1969) Discharge properties of Purkinje cells recorded on single and double microelectrodes. J. Neurophysiol. 32: 1044–1055.

Bower JM (1997a) Control of sensory data acquisition. International Review of Neurobiology 41: 489–513.

Bower JM (1997b) Is the cerebellum sensory for motor's sake, or motor for sensory's sake: The view from the whiskers of a rat? Prog. Brain. Res. 114: 483–516.

Bower JM, Beeman D (1994) The Book of Genesis. Springer, New York.

Bower JM, Woolston DC (1983) Congruence of spatial organization of tactile projections to granule cell and Purkinje cell layers of cerebellar hemispheres of the albino rat: Vertical organization of cerebellar cortex. J. Neurophysiol. 49: 745–766.

Braitenberg V (1967) Is the cerebellar cortex a biological clock in the millisecond range? Prog. Brain. Res. 25: 334–346.

Braitenberg V, Atwood RP (1958) Morphological observations on the cerebellar cortex. J. Comp. Neurol. 109: 1–33.

Braitenberg V, Heck D, Sultan F (1997) The detection and generation of sequences as a key to cerebellar function: Experiments and theory. Behav. Brain Sci. 20: 229–277.

Brody CD (1999) Correlations withouth synchrony. Neural Comp. 11: 1537–1551.

Cohen D, Yarom Y (1998) Patches of synchronized activity in the cerebellar cortex evoked by mossy-fiber stimulation: Questioning the role of parallel fibers. Proc. Natl. Acad. Sci. USA 95: 15032–15036.

Crepel F, Dhanjal SS, Garthwaite J (1981) Morphological and electrophysiological characteristics of rat cerebellar slices maintained in vitro. J. Physiol. (Lond.) 316: 127–138.

De Schutter E (1998) Dendritic voltage and calcium-gated channels amplify the variability of postsynaptic responses in a Purkinje cell model. J. Neurophysiol. 80: 504–519.

De Schutter E, Bower JM (1994a) An active membrane model of the cerebellar Purkinje cell I. Simulation of current clamp in slice. J. Neurophysiol. 71: 375–400.

De Schutter E, Bower JM (1994b) An active membrane model of the cerebellar Purkinje cell. II. Simulation of synaptic responses. J. Neurophysiol. 71: 401–419.

De Schutter E, Bower JM (1994c) Simulated responses of cerebellar Purkinje cells are independent of the dendritic location of granule cell synaptic inputs. Proc. Natl. Acad. Sci. USA 91: 4736–4740.

Diesmann M, Gewaltig MO, Aertsen A (1999) Stable propagation of synchronous spiking in cortical neural networks. Nature 402: 529–533.

Dugas C, Smith AM (1992) Responses of cerebellar Purkinje cells to slip of a hand-held object. J. Neurophysiol. 67: 483–495.

Ebner TJ, Bloedel JR (1981) Correlation between activity of Purkinje cells and its modification by natural peripheral stimuli. J. Neurophysiol. 45: 948–961.

Eccles JC, Sasaki K, Strata P (1967) Interpretation of the field potentials generated in the cerebellar cortex by a mossy fibre volley. Exp. Brain Res. 3: 58–80.

Fortier PA, Kalaska JF, Smith AM (1989) Cerebellar neuronal activity related to whole-arm reaching movements in the monkey. J. Neurophysiol. 62: 198–211.

Garwicz M, Andersson G (1992) Spread of synaptic activity along parallel fibres in cat cerebellar anterior lobe. Exp. Brain Res. 88: 615–622.

Gauck V, Jaeger D (2000) The control of rate and timing of spikes in the deep cerebellar nuclei by inhibition. J. Neurosci. 20: 3006–3016.

Hartmann MJ, Bower JM (1998) Oscillatory activity in the cerebellar hemispheres of unrestrained rats. J. Neurophysiol. 80: 1598–1604.

Hartmann MJ, Bower JM (2001) Tactile responses in the granule cell layer of cerebellar folium Crus IIa of freely behaving rats. J. Neurosci. 21: 3549–3563.

Harvey RJ, Napper RMA (1991) Quantitative studies of the mammalian cerebellum. Prog. Neurobiol. 36: 437–463.

Häusser M, Clark BA (1997) Tonic synaptic inhibition modulates neuronal output pattern and spatiotemporal synaptic integration. Neuron 19: 665–678.

Houk JC, Buckingham JT, Barto AG (1996) Models of the cerebellum and motor learning. Behav. Brain Sci. 19: 368–383.

Huang C-M, Mu H, Hsiao C-F (1993) Identification of cell types from action potential waveforms: Cerebellar granule cells. Brain Res. 619: 313–318.

Isope P, Barbour P. (2001) The majority of granule cell Purkinje cell synapses are silent. Soc. Neurosci. Abstr. 27: Program No. 713.5.

Ito M (1984) The Cerebellum and Neural Control. Raven Press, New York.

Ivry R (1997) Cerebellar timing systems. Int. Rev. Neurobiol. 41: 555–573.

Jaeger D, Bower JM (1994) Prolonged responses in rat cerebellar Purkinje cells following activation of the granule cell layer: An intracellular in vitro and in vivo investigation. Exp. Brain Res. 100: 200–214.

Jaeger D, Bower JM (1999) Synaptic control of spiking in cerebellar Purkinje cells: Dynamic current clamp based on model conductances. J. Neurosci 19: 6090–6101.

Jaeger D, De Schutter E, Bower JM (1997) The role of synaptic and voltage-gated currents in the control of Purkinje cell spiking: A modeling study. J. Neurosci 17: 91–106.

Johnson MJ, Alloway KD (1996) Cross-correlation analysis reveals laminar differences in thalamocortical interactions in the somatosensory system. J. Neurophysiol. 75: 1444–1457.

Lang EJ, Sugihara I, Welsh JP, Llinás R (1999) Patterns of spontaneous Purkinje cell complex spike activity in the awake rat. J. Neurosci. 19: 2728–2739.

Lisberger SG, Fuchs AF (1978) Role of primate flocculus during rapid behavioral modification of vestiubloocular reflex. I. Purkinje cell activity during visually guided horizontal smooth-pursuit eye movements and passive head rotation. J. Neurophysiol. 41: 733–763.

Llinás R (1982) General discussion: Radial connectivity in the cerebellar cortex: A novel view regarding the functional organization of the molecular layer. In: SL Palay, V Chan-Palay, eds. The Cerebellum: New Vistas, (Exp. Brain Res. Suppl. Vol. 6). Springer Verlag, New York. pp. 189–194.

Llinás R, Sugimori M (1980) Electrophysiological properties of in vitro Purkinje cell somata in mammalian cerebellar slices. J. Physiol. (Lond.) 305: 171–195.

Mano N, Ito Y, Shibutani H (1991) Saccade-related Purkinje cells in the cerebellar hemispheres of the monkey. Exp. Brain Res. 84: 465–470.

Mano N-I, Yamamoto K-I (1980) Simple-spike activity of cerebellar Purkinje cells related to visually guided wrist tracking movement in the monkey. J. Neurophysiol. 43: 713–728.

Mauk MD, Garcia KS, Medina JF, Steele PM (1998) Does cerebellar LTD mediate motor learning? Toward a resolution without a smoking gun. Neuron 20: 359–362.

Medina JF, Mauk MD (2000) Computer simulation of cerebellar information processing. Nat. Neurosci. 3: 1205–1211.

Moore GP, Segundo JP, Perkel DH, Levitan H (1970) Statistical signs of synaptic interaction in neurons. Biophys. J. 10: 876–900.

Napper RMA, Harvey RJ (1988) Number of parallel fiber synapses on an individual Purkinje cell in the cerebellum of the rat. J. Comp. Neurol. 274: 168–177.

Palkovits M, Magyar P, Szentagothai J (1971) Quantitative histological analysis of the cerebellar cortex in the cat. III. Structural organization of the molecular layer. Brain Res. 34: 1–18.

Palm G, Aertsen AM, Gerstein GL (1988) On the significance of correlations among neuronal spike trains. Biol. Cybern. 59: 1–11.

Perkel DH, Gerstein GL, Moore GP (1967) Neuronal spike trains and stochastic point processes. II Simultaneous spike trains. Biophys. J. 7: 419–440.

Rapp M, Yarom Y, Segev I (1992) The impact of parallel fiber background activity on the cable properties of cerebellar Purkinje cells. Neural Comput. 4: 518–533.

Riehle A, Grün S, Diesmann M, Aertsen A (1997) Spike synchronization and rate modulation differentially involved in motor cortical function. Science 278: 1950–1953.

Santamaria F, Jaeger D, De Schutter E, Bower JM (2002) Modulatory effects of parallel fibers and stellate cell synaptic activity on Purkinje cell responses to ascending segment input: A modeling study. J. Comput. Neurosci. 13: 217–235.

Sasaki K, Strata P (1967) Responses evoked in the cerebellar cortex by stimulating mossy fibre pathways to the cerebellum. Experimental Brain Research 3: 95–110.

Savio T, Tempia F (1985) On the Purkinje cell activity increase induced by suppression of inferior olive activity. Exp. Brain Res. 57: 456–463.

Singer W (1999) Neuronal synchrony: A versatile code for the definition of relations? Neuron 24: 49–65.

Stratton SE, Lorden JF, Mays LE, Oltmans GA (1988) Spontaneous and harmaline-stimulated Purkinje cell activity in rats with a genetic movement disorder. J. Neurosci. 8: 3327–3336.

Timmann D, Watts S, Hore J (1999) Failure of cerebellar patients to time finger opening precisely causes ball high-low inaccuracy in overarm throws. J. Neurophysiol. 82: 103–114.

Vaadia E, Haalman I, Abeles M, Bergman YP, Slovin H, Aertsen A (1995) Dynamics of neuronal interactions in monkey cortex in relation to behavioural events. Nature 373: 515–518.

Welsh JP, Lang EJ, Sugihara I, Llinás R (1995) Dynamic organization of motor control within the olivocerebellar system. Nature 374: 453–457.

Williams SR, Christensen SR, Stuart GJ, Hausser M (2002) Membrane potential bistability is controlled by the hyperpolarization-activated current I(H) in rat cerebellar Purkinje neurons in vitro. J. Physiol 539: 469–483.